Journal of Engineering Mathematics, Vol. 12, No. 2, April 1978
Sijthoff & Noordhoff International Publishers–Alphen aan den Rijn
Printed in The Netherlands

A differential-equation method for the computation of the electromagnetic scattering by an inhomogeneity in a cylindrical waveguide

G. MUR

Department of Electrical Engineering, Laboratory of Electromagnetic Research, Delft University of Technology, Mekelweg 4, Delft-2208, The Netherlands.

(Received June 3, 1977)

SUMMARY

In this paper an exact method is described for computing numerically the scattering by an inhomogeneity in a cylindrical waveguide. The "Generalized Telegraphist's Equations" are used to transform the electromagnetic-field equations into a system of ordinary differential equations. The latter system behaves numerically unstable. A method is given to cope with this difficulty. Numerical results are presented for two- and three-dimensional obstacles in a waveguide of rectangular cross-section and they are compared with those obtained by other methods. Our method requires, in general, a relatively small amount of computation time and storage capacity. Another advantage of the method is its flexibility.

1. Introduction

In this paper an exact method is described for computing numerically the electromagnetic scattering properties of an inhomogeneity in the dielectric and/or the magnetic properties of the medium in an otherwise uniform, cylindrical waveguide (Fig. 1). In the waveguide, three different regions are distinguished, viz. the Regions 1 and 3 in which the medium is homogeneous and Region 2 in which the inhomogeneity in the properties of the medium is located. In the homogeneous regions of the waveguide, the fields can be expressed in terms of an uncoupled system of *TE*-, *TM*- and, if present, *TEM*-modes. In Region 2, where the inhomogeneity is located the "Generalized Telegraphist's Equations" [1] are used to transform Maxwell's partial differential equations into an infinite system of ordinary

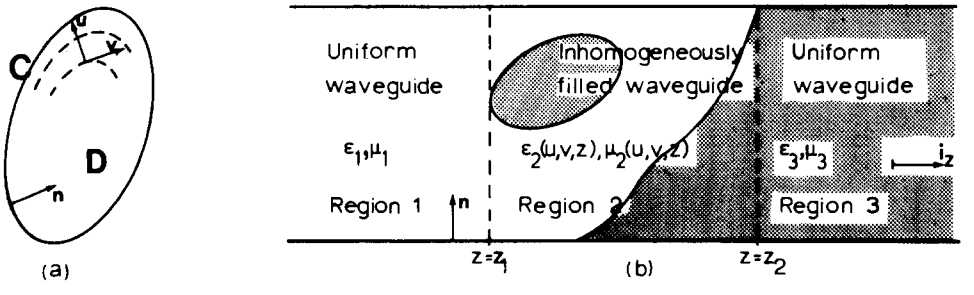

Figure 1. Cross-section (a) and longitudinal section (b) of the waveguide configuration.

differential equations in z, the longitudinal coordinate. The presence of the inhomogeneity causes these differential equations to be coupled through z-dependent coupling coefficients. At either boundary between a homogeneous and the inhomogeneous region, continuity conditions apply. The relevant system of differential equations appears to be numerically unstable. In Section 4 we present a method to transform the system of differential equations into a related one with better stability properties as regards its numerical solution. To illustrate the applicability of the method, the scattering properties of obstacles of varying complexity, present in a waveguide with rectangular cross-section, are computed. The results are presented in Section 6.

The hitherto-known methods that deal with scattering problems of the type under consideration, are either approximate in nature, such as quasi-static approximations [2], or exact, using an integral-equation formulation of the problem [3, 4, 5]. Although being exact, integral-equation methods have the disadvantage that they require the (often very time consuming) evaluation of dyadic Green's functions, and, in general, a large amount of storage capacity. Our method of solution is exact, too, but requires only a relatively small amount of computer time and storage capacity [6].

2. Description of the configuration

The configuration under consideration (Fig. 1) consists of the three different regions that are defined in Table 1. In this table, also the permittivity ε and the permeability μ applying to these regions are indicated, as well as the relevant wavenumbers. We shall consider time-harmonic fields. The complex time factor $\exp(j\omega t)$, where j = imaginary unit, ω denotes the angular frequency and t the time, is omitted in the formulas. Since the media in the waveguide may be lossy, the constitutive coefficients are in general complex with a negative imaginary part.

TABLE 1
Regions in the waveguide.

Region	Location $(u, v) \in D$	Constitutive coefficients ε, μ of the medium	Wavenumber $\mathrm{Re}(k) > 0$
Region 1	$-\infty < z < z_1$	$\varepsilon_0\varepsilon_1$, $\mu_0\mu_1$	$k_1 = k_0(\varepsilon_1\mu_1)^{\frac{1}{2}}$
Region 2	$z_1 < z < z_2$	$\varepsilon_0\varepsilon_2(u, v, z)$, $\mu_0\mu_2(u, v, z)$	$k_2 = k_0(\varepsilon_2\mu_2)^{\frac{1}{2}}$
Region 3	$z_2 < z < \infty$	$\varepsilon_0\varepsilon_3$, $\mu_0\mu_3$	$k_3 = k_0(\varepsilon_3\mu_3)^{\frac{1}{2}}$

ε_0 and μ_0 denote the permittivity and the permeability respectively, of the reference medium; $k_0 = \omega(\varepsilon_0\mu_0)^{\frac{1}{2}} > 0$ denotes the wavenumber in the reference medium.

The electromagnetic fields in the configuration satisfy the source-free electromagnetic-field equations

$$\nabla \times \boldsymbol{H} = j\omega\varepsilon\boldsymbol{E}, \quad \nabla \times \boldsymbol{E} = -j\omega\mu\boldsymbol{H}, \tag{1}$$

where $\varepsilon = \varepsilon(\boldsymbol{r})$ and $\mu = \mu(\boldsymbol{r})$ denote the local value of the permittivity and the permeability, respectively. The waveguide wall is assumed to be perfectly conducting and on it the

boundary condition

$$\boldsymbol{n} \times \boldsymbol{E} = \boldsymbol{0} \tag{2}$$

holds ($\boldsymbol{n}$ denotes the unit vector along the normal to the waveguide wall, as shown in Fig. 1).

3. Derivation of the "Generalized Telegraphist's Equations"

As has been stated in the introduction, we shall in Region 2, where the inhomogeneity is present, transform the electromagnetic-field equations into a system of "Generalized Telegraphist's Equations". In the derivation of these equations we shall closely follow the line of thought due to Schelkunoff [1]. Thus, we first consider the modes of propagation in a guide filled with a homogeneous reference medium, not necessarily being vacuum. Each mode in this waveguide is described by the transverse distribution pattern T of either a potential or a stream function. To indicate the distinction between *TE*- and *TM*-modes we follow the convention adopted in [1], where the ordinal numbers for *TE*-modes are enclosed in brackets and those for *TM*-modes in parentheses. The *TEM*-modes will be treated as a special case of the *TM*-modes. For convenience, we use a single-subscript notation, while arranging the modes in the order of non-decreasing cut-off frequencies. The function $T(u, v)$, where u and v are suitable coordinates in a cross-section D with boundary C (see Fig. 1), is a solution of the two-dimensional Helmholtz equation in the cross-sectional domain. For *TE*-modes we have

$$(\nabla_T^2 + \kappa_{[n]}^2) T_{[n]} = 0 \qquad \text{in } D, \tag{3}$$

together with the boundary condition

$$\partial_n T_{[n]} = 0 \qquad \text{on } C. \tag{4}$$

In (3), $\kappa_{[n]}$ denotes the (real) cut-off wavenumber of the n-th *TE*-mode, while $\nabla_T = \nabla - \boldsymbol{i}_z \partial_z$. For *TM*-modes we have

$$(\nabla_T^2 + \kappa_{(n)}^2) T_{(n)} = 0 \qquad \text{in } D, \tag{5}$$

together with the boundary condition

$$T_{(n)} = 0 \qquad \text{on } C. \tag{6}$$

In (5), $\kappa_{(n)}$ denotes the (real) cut-off wavenumber of the n-th *TM*-mode. The T-functions, that are chosen to be real, satisfy a number of orthogonality relations that are given in [1]; they are normalized such that

$$\begin{aligned} \iint_D (\nabla_T T_{[n]}) \cdot (\nabla_T T_{[n]}) \mathrm{d}A &= \kappa_{[n]}^2 \iint_D T_{[n]}^2 \mathrm{d}A = 1, \\ \iint_D (\nabla_T T_{(n)}) \cdot (\nabla_T T_{(n)}) \mathrm{d}A &= \kappa_{(n)}^2 \iint_D T_{(n)}^2 \mathrm{d}A = 1. \end{aligned} \tag{7}$$

The transverse components $\boldsymbol{E}_T$ and $\boldsymbol{H}_T$ of the electric- and the magnetic-field strength, respectively can be expressed in terms of the potential and stream functions, Ψ and U for TE-modes, V and Π for TM-modes, as

$$\boldsymbol{E}_T = -\nabla_T V + \boldsymbol{i}_z \times \nabla_T \Psi, \quad \boldsymbol{H}_T = -\nabla_T U - \boldsymbol{i}_z \times \nabla_T \Pi \tag{8}$$

where $\boldsymbol{i}_z$ denotes the unit vector in the direction of increasing z. In general, the potential and stream functions can be written as

$$\begin{aligned} \Psi(u, v, z) &= -\sum_n V_{[n]}(z) T_{[n]}(u, v), \quad U(u, v, z) = -\sum_n I_{[n]}(z) T_{[n]}(u, v), \\ V(u, v, z) &= -\sum_n V_{(n)}(z) T_{(n)}(u, v), \quad \Pi(u, v, z) = -\sum_n I_{(n)}(z) T_{(n)}(u, v), \end{aligned} \tag{9}$$

where the minus signs have been inserted to avoid a preponderance of minus signs in later equations. The V's and the I's of a mode represent the "voltages" and the "currents" in the equivalent transmission lines. Substituting (9) in (8) we obtain

$$\begin{aligned} \boldsymbol{E}_T &= \sum_n (V_{(n)}(z) \nabla_T T_{(n)}(u, v) - \boldsymbol{i}_z \times V_{[n]}(z) \nabla_T T_{[n]}(u, v)), \\ \boldsymbol{H}_T &= \sum_n (I_{[n]}(z) \nabla_T T_{[n]}(u, v) + \boldsymbol{i}_z \times I_{(n)}(z) \nabla_T T_{(n)}(u, v)). \end{aligned} \tag{10}$$

We note that in obtaining (10), the medium in the reference waveguide, apart from being homogeneous, has not been specified. Furthermore we note that the expansion (10) of the transverse field components $\boldsymbol{E}_T$ and $\boldsymbol{H}_T$ is in terms of a complete sequence of transverse field distributions.

Having derived general expressions for the transverse field components in the reference waveguide, we now consider the fields in Region 2. To obtain expressions for the transverse field components in this region, we separate the transverse field components in the electromagnetic-field equations (1) from the axial ones and write the result as

$$\begin{aligned} \partial_z \boldsymbol{H}_T &= \nabla_T H_z - \mathrm{j}\omega\varepsilon \boldsymbol{i}_z \times \boldsymbol{E}_T, \quad \partial_z \boldsymbol{E}_T = \nabla_T E_z + \mathrm{j}\omega\mu \boldsymbol{i}_z \times \boldsymbol{H}_T, \\ E_z &= (\mathrm{j}\omega\varepsilon)^{-1} \nabla_T \cdot (\boldsymbol{H}_T \times \boldsymbol{i}_z), \quad H_z = (\mathrm{j}\omega\mu)^{-1} \nabla_T \cdot (\boldsymbol{i}_z \times \boldsymbol{E}_T). \end{aligned} \tag{11}$$

As a consequence of the completeness of the sequence of expansion functions, the expression (10) for $\boldsymbol{E}_T$ and $\boldsymbol{H}_T$ can also be used in Region 2. Substituting (10) in (11) and eliminating the longitudinal field components E_z and H_z we obtain

$$\begin{aligned} &\sum_n (\partial_z I_{[n]}) \nabla_T T_{[n]} + \sum_n (\partial_z I_{(n)}) \boldsymbol{i}_z \times \nabla_T T_{(n)} \\ &\quad = -\mathrm{j}\omega\varepsilon \sum_n (V_{(n)} \boldsymbol{i}_z \times \nabla_T T_{(n)} + V_{[n]} \nabla_T T_{[n]}) - \sum_n \kappa_{[n]}^2 V_{[n]} \nabla_T ((\mathrm{j}\omega\mu)^{-1} T_{[n]}), \end{aligned} \tag{12}$$

$$\begin{aligned} &\sum_n (\partial_z V_{(n)}) \nabla_T T_{(n)} - \sum_n (\partial_z V_{[n]}) \boldsymbol{i}_z \times \nabla_T T_{[n]} \\ &\quad = \mathrm{j}\omega\mu \sum_n (I_{[n]} \boldsymbol{i}_z \times \nabla_T T_{[n]} - I_{(n)} \nabla_T T_{(n)}) - \sum_n \kappa_{(n)}^2 I_{(n)} \nabla_T ((\mathrm{j}\omega\varepsilon)^{-1} T_{(n)}). \end{aligned} \tag{13}$$

We now perform the following operations. First, we carry out a scalar multiplication of (13) by the vector functions $\boldsymbol{i}_z \times \nabla_T T_{[m]}$ and $\nabla_T T_{(m)}$, respectively. Secondly, we carry out a scalar multiplication of (12) by the vector functions $\nabla_T T_{[m]}$ and $\boldsymbol{i}_z \times \nabla_T T_{(m)}$, respectively. Subsequently, we integrate the four resulting equations over the cross-section D of the waveguide. As a result we obtain, using the orthogonality relations of the T-functions and the normalization conditions (7), a system of differential equations that can be written as [1]

$$\begin{aligned}
-\partial_z V_{[m]}(z) &= \sum_n (Z_{[m][n]}(z) I_{[n]}(z) + Z_{[m](n)}(z) I_{(n)}(z)),\\
-\partial_z V_{(m)}(z) &= \sum_n (Z_{(m)[n]}(z) I_{[n]}(z) + Z_{(m)(n)}(z) I_{(n)}(z)),\\
-\partial_z I_{[m]}(z) &= \sum_n (Y_{[m][n]}(z) V_{[n]}(z) + Y_{[m](n)}(z) V_{(n)}(z)),\\
-\partial_z I_{(m)}(z) &= \sum_n (Y_{(m)[n]}(z) V_{[n]}(z) + Y_{(m)(n)}(z) V_{(n)}(z)),
\end{aligned} \qquad \text{in Region 2} \quad (14)$$

with

$$\begin{aligned}
Z_{[m][n]}(z) &= \mathrm{j}\omega\mu_0 \iint_D \mu_2 (\boldsymbol{i}_z \times \nabla_T T_{[m]}) \cdot (\boldsymbol{i}_z \times \nabla_T T_{[n]}) \mathrm{d}A,\\
Z_{[m](n)}(z) &= -\mathrm{j}\omega\mu_0 \iint_D \mu_2 (\boldsymbol{i}_z \times \nabla_T T_{[m]}) \cdot \nabla_T T_{(n)} \mathrm{d}A,\\
Z_{(m)[n]}(z) &= -\mathrm{j}\omega\mu_0 \iint_D \mu_2 \nabla_T T_{(m)} \cdot (\boldsymbol{i}_z \times \nabla_T T_{[n]}) \mathrm{d}A,\\
Z_{(m)(n)}(z) &= \mathrm{j}\omega\mu_0 \iint_D \mu_2 \nabla_T T_{(m)} \cdot \nabla_T T_{(n)} \mathrm{d}A + \kappa_{(m)}^2 \kappa_{(n)}^2 \iint_D (\mathrm{j}\omega\varepsilon_0\varepsilon_2)^{-1} T_{(m)} T_{(n)} \mathrm{d}A,
\end{aligned} \qquad (15)$$

and

$$\begin{aligned}
Y_{[m][n]}(z) &= \mathrm{j}\omega\varepsilon_0 \iint_D \varepsilon_2 \nabla_T T_{[m]} \cdot \nabla_T T_{[n]} \mathrm{d}A + \kappa_{[m]}^2 \kappa_{[n]}^2 \iint_D (\mathrm{j}\omega\mu_0\mu_2)^{-1} T_{[m]} T_{[n]} \mathrm{d}A,\\
Y_{[m](n)}(z) &= \mathrm{j}\omega\varepsilon_0 \iint_D \varepsilon_2 \nabla_T T_{[m]} \cdot (\boldsymbol{i}_z \times \nabla_T T_{(n)}) \mathrm{d}A,\\
Y_{(m)[n]}(z) &= \mathrm{j}\omega\varepsilon_0 \iint_D \varepsilon_2 (\boldsymbol{i}_z \times \nabla_T T_{(m)}) \cdot \nabla_T T_{[n]} \mathrm{d}A,\\
Y_{(m)(n)}(z) &= \mathrm{j}\omega\varepsilon_0 \iint_D \varepsilon_2 (\boldsymbol{i}_z \times \nabla_T T_{(m)}) \cdot (\boldsymbol{i}_z \times \nabla_T T_{(n)}) \mathrm{d}A.
\end{aligned} \qquad (16)$$

Now, (14) constitutes the system of generalized telegraphist's equations for the inhomogeneity in Region 2. These first-order ordinary differential equations are to be supplemented by boundary conditions at the planes $z = z_1$ and $z = z_2$ bounding the waveguide section in which the inhomogeneity is located. Across these planes the tangential field components $\boldsymbol{E}_T$ and $\boldsymbol{H}_T$ are continuous. In order to formulate the relevant boundary conditions we must first obtain expressions for the transverse field components in Region 1 and Region 3.

In Region 1 we assume that the field consists of incident modes travelling in the positive z-direction, having a voltage V^i and a current I^i, and scattered modes travelling in the negative z-direction having a voltage V^s and a current I^s. The transverse field in Region 1 can therefore be written as

$$\begin{aligned} \boldsymbol{E}_T &= \sum_m (V^i_{1,(m)} + V^s_{1,(m)})\nabla_T T_{(m)} \\ &\quad - \boldsymbol{i}_z \times \sum_m (V^i_{1,[m]} + V^s_{1,[m]})\nabla_T T_{[m]}, \\ \boldsymbol{H}_T &= \sum_m (I^i_{1,[m]} + I^s_{1,[m]})\nabla_T T_{[m]} \\ &\quad + \boldsymbol{i}_z \times \sum_m (I^i_{1,(m)} + I^s_{1,(m)})\nabla_T T_{(m)}. \end{aligned} \qquad \text{in Region 1} \qquad (17)$$

The voltages and the currents of these (uncoupled) modes are related through

$$\begin{aligned} V^i_{1,[m]} &= Z_{1,[m]} I^i_{1,[m]}, \qquad V^s_{1,[m]} = -Z_{1,[m]} I^s_{1,[m]}, \\ V^i_{1,(m)} &= Z_{1,(m)} I^i_{1,(m)}, \qquad V^s_{1,(m)} = -Z_{1,(m)} I^s_{1,(m)}. \end{aligned} \qquad (18)$$

In (18), $Z_{1,[m]}$ and $Z_{1,(m)}$ denote the wave impedances of the m-th TE- and TM-mode in Region 1, respectively. We have

$$Z_{1,[m]} = \mathrm{j}\omega\mu_0\mu_1/\Gamma_{1,[m]}, \qquad Z_{1,(m)} = \Gamma_{1,(m)}/\mathrm{j}\omega\varepsilon_0\varepsilon_1, \qquad (19)$$

where $\Gamma_{1,[m]}$ and $\Gamma_{1,(m)}$ denote the propagation coefficients of the m-th TE- and TM-mode in Region 1, respectively, i.e.

$$\begin{aligned} \Gamma_{1,[m]} &= (\kappa^2_{[m]} - k_1^2)^{\frac{1}{2}} \text{ with } \mathrm{Im}(\Gamma_{1,[m]}) \geq 0, \\ \Gamma_{1,(m)} &= (\kappa^2_{(m)} - k_1^2)^{\frac{1}{2}} \text{ with } \mathrm{Im}(\Gamma_{1,(m)}) \geq 0. \end{aligned} \qquad (20)$$

The propagation factor of a mode is $\exp(-\Gamma z)$. In Region 3, the field consists of incident waves travelling in the negative z-direction and scattered waves travelling in the positive z-direction. The transverse fields in Region 3 are written as

$$\begin{aligned} \boldsymbol{E}_T &= \sum_m (V^i_{3,(m)} + V^s_{3,(m)})\nabla_T T_{(m)} \\ &\quad - \boldsymbol{i}_z \times \sum_m (V^i_{3,[m]}) + V^s_{3,[m]})\nabla_T T_{[m]}, \\ \boldsymbol{H}_T &= \sum_m (I^i_{3,[m]} + I^s_{3,[m]})\nabla_T T_{[m]} \\ &\quad + \boldsymbol{i}_z \times \sum_m (I^i_{3,(m)} + I^s_{3,(m)})\nabla_T T_{(m)}, \end{aligned} \qquad \text{in Region 3} \qquad (21)$$

where the voltages and the currents are related through

$$\begin{aligned} V^i_{3,[m]} &= -Z_{3,[m]} I^i_{3,[m]}, \qquad V^s_{3,[m]} = Z_{3,[m]} I^s_{3,[m]}, \\ V^i_{3,(m)} &= -Z_{3,(m)} I^i_{3,(m)}, \qquad V^s_{3,(m)} = Z_{3,(m)} I^s_{3,(m)}. \end{aligned} \qquad (22)$$

In (22), $Z_{3,[m]}$ and $Z_{3,(m)}$ denote the wave impedances of the m-th *TE*- and *TM*-mode in Region 3, respectively, i.e.

$$Z_{3,[m]} = \mathrm{j}\omega\mu_0\mu_3/\Gamma_{3,[m]}, \qquad Z_{3,(m)} = \Gamma_{3,(m)}/\mathrm{j}\omega\varepsilon_0\varepsilon_3, \tag{23}$$

where $\Gamma_{3,[m]}$ and $\Gamma_{3,(m)}$ denote the propagation coefficients of the m-th *TE*- and *TM*-mode in Region 3, respectively, with

$$\begin{aligned} &\Gamma_{3,[m]} = (\kappa_{[m]}^2 - k_3^2)^{\frac{1}{2}} \text{ with } \mathrm{Im}(\Gamma_{3,[m]}) \geq 0, \\ &\Gamma_{3,(m)} = (\kappa_{(m)}^2 - k_3^2)^{\frac{1}{2}} \text{ with } \mathrm{Im}(\Gamma_{3,(m)}) \geq 0. \end{aligned} \tag{24}$$

Now we derive the boundary conditions pertaining to the system of differential equations (14). Taking the limit $z \downarrow z_1$ in (10) and $z \uparrow z_1$ in (17), using the continuity of the tangential field components at the plane $z = z_1$ and the orthogonality properties of the T-functions we arrive at

$$\begin{aligned} &V_{[m]}(z_1) = V_{1,[m]}^i(z_1) + V_{1,[m]}^s(z_1), \quad V_{(m)}(z_1) = V_{1,(m)}^i(z_1) + V_{1,(m)}^s(z_1), \\ &I_{[m]}(z_1) = I_{1,[m]}^i(z_1) + I_{1,[m]}^s(z_1), \quad I_{(m)}(z_1) = I_{1,(m)}^i(z_1) + I_{1,(m)}^s(z_1). \end{aligned} \tag{25}$$

Eliminating the scattered fields from (25) by using (18), we obtain the boundary conditions

$$V_{[m]}(z_1) + Z_{1,[m]}I_{[m]}(z_1) = 2V_{1,[m]}^i(z_1), \quad V_{(m)}(z_1) + Z_{1,(m)}I_{(m)}(z_1) = 2V_{1,(m)}^i(z_1). \tag{26}$$

In the same way, using (10), (21) and (22), we obtain at $z = z_2$ the boundary conditions

$$V_{[m]}(z_2) - Z_{3,[m]}I_{[m]}(z_2) = 2V_{3,[m]}^i(z_2), \quad V_{(m)}(z_2) - Z_{3,(m)}I_{(m)}(z_2) = 2V_{3,(m)}^i(z_2). \tag{27}$$

Now (14), together with the boundary conditions (26) and (27), constitutes a two-point boundary-value problem. After having solved this boundary-value problem, the scattered fields in the Regions 1 and 3 can be computed by again using the continuity conditions (25) and the corresponding conditions at the boundary plane $z = z_2$.

The numerical solution of the two-point boundary-value problem could be obtained by using standard techniques, for instance by using a shooting method in which case the problem is replaced by a related initial-value problem [7, 8]. However, the corresponding initial-value problem turns out to be numerically unstable [6]. Consequently, in this way only inhomogeneities of relatively small axial dimensions can be investigated (in general the axial dimension should be smaller than the transverse dimension of the guide). In Section 4 we shall transform the present two-point boundary-value problem into a different boundary-value problem, the latter having the advantage of leading to an associated initial-value problem that is stable.

4. Transformation of the system of differential equations into a stable one

In order to cope with the stability problems posed by the numerical solution of (14), we introduce new z-dependent potential functions $V^{\pm}_{[m]}$ and $V^{\pm}_{(m)}$ that are defined as follows

$$\begin{aligned} V^{\pm}_{[m]}(z) &= \tfrac{1}{2}(V_{[m]}(z) \pm Z_{[m]}I_{[m]}(z)), \\ V^{\pm}_{(m)}(z) &= \tfrac{1}{2}(V_{(m)}(z) \pm Z_{(m)}I_{(m)}(z)). \end{aligned} \qquad \text{in Region 2} \qquad (28)$$

In (28), $Z_{[m]}$ and $Z_{(m)}$ denote the wave impedances of the m-th TE- and TM-mode, respectively, in the homogeneous reference waveguide. For the impedances and the admittances of the modes in the reference waveguide we have

$$Z_{[m]} = Y^{-1}_{[m]} = \mathrm{j}\omega\mu_0/\Gamma_{[m]}, \qquad Z_{(m)} = Y^{-1}_{(m)} = \Gamma_{(m)}/\mathrm{j}\omega\varepsilon_0, \qquad (29)$$

where $\Gamma_{[m]}$ and $\Gamma_{(m)}$ denote the propagation coefficients of the m-th TE- and TM-mode in the homogeneous reference waveguide, respectively. We have

$$\begin{aligned} \Gamma_{[m]} &= (\kappa^2_{[m]} - k_0^2)^{\frac{1}{2}} \text{ with } \mathrm{Im}(\Gamma_{[m]}) \geq 0, \\ \Gamma_{(m)} &= (\kappa^2_{(m)} - k_0^2)^{\frac{1}{2}} \text{ with } \mathrm{Im}(\Gamma_{(m)}) \geq 0. \end{aligned} \qquad (30)$$

At this point we observe that the permittivity ε_0 and the permeability μ_0 of the reference medium can still arbitrarily be chosen. The differential equations to be satisfied by $V^{\pm}_{[m]}$ and $V^{\pm}_{(m)}$ are obtained from (14) and (28) as

$$\begin{aligned} -2\partial_z V^{\pm}_{[m]}(z) = &\sum_n (Z_{[m][n]}Y_{[n]} \pm Z_{[m]}Y_{[m][n]})V^{+}_{[n]} \\ &+ \sum_n (-Z_{[m][n]}Y_{[n]} \pm Z_{[m]}Y_{[m][n]})V^{-}_{[n]} \\ &+ \sum_n (Z_{[m](n)}Y_{(n)} \pm Z_{[m]}Y_{[m](n)})V^{+}_{(n)} \\ &+ \sum_n (-Z_{[m](n)}Y_{(n)} \pm Z_{[m]}Y_{[m](n)})V^{-}_{(n)}, \\ -2\partial_z V^{\pm}_{(m)}(z) = &\sum_n (Z_{(m)[n]}Y_{[n]} \pm Z_{(m)}Y_{(m)[n]})V^{+}_{[n]} \\ &+ \sum_n (-Z_{(m)[n]}Y_{[n]} \pm Z_{(m)}Y_{(m)[n]})V^{-}_{[n]} \\ &+ \sum_n (Z_{(m)(n)}Y_{(n)} \pm Z_{(m)}Y_{(m)(n)})V^{+}_{(n)} \\ &+ \sum_n (-Z_{(m)(n)}Y_{(n)} \pm Z_{(m)}Y_{(m)(n)})V^{-}_{(n)}. \end{aligned} \qquad \text{in Region 2} \qquad (31)$$

The corresponding transformation of the boundary conditions (26) and (27) leads to

$$\begin{aligned} (1 + Z_{1,[m]}Y_{[m]})V^{+}_{[m]}(z_1) + (1 - Z_{1,[m]}Y_{[m]})V^{-}_{[m]}(z_1) &= 2V^{i}_{1,[m]}(z_1), \\ (1 + Z_{1,(m)}Y_{(m)})V^{+}_{(m)}(z_1) + (1 - Z_{1,(m)}Y_{(m)})V^{-}_{(m)}(z_1) &= 2V^{i}_{1,(m)}(z_1), \end{aligned} \qquad (32)$$

and

$$\begin{aligned}(1 - Z_{3,[m]}Y_{[m]})V^{+}_{[m]}(z_2) + (1 + Z_{3,[m]}Y_{[m]})V^{-}_{[m]}(z_2) &= 2V^{i}_{3,[m]}(z_2),\\ (1 - Z_{3,(m)}Y_{(m)})V^{+}_{(m)}(z_2) + (1 + Z_{3,(m)}Y_{(m)})V^{-}_{(m)}(z_2) &= 2V^{i}_{3,(m)}(z_2).\end{aligned} \tag{33}$$

The two-point boundary-value problem defined by the system of differential equations (31), together with the boundary conditions (32) and (33), can again be solved by using a shooting method. The initial-value problem obtained in this case turns out to be numerically stable. The related scattered field is obtained from

$$\begin{aligned}V^{s}_{1,[m]}(z_1) &= V^{+}_{[m]}(z_1) + V^{-}_{[m]}(z_1) - V^{i}_{1,[m]}(z_1),\\ V^{s}_{1,(m)}(z_1) &= V^{+}_{(m)}(z_1) + V^{-}_{(m)}(z_1) - V^{i}_{1,(m)}(z_1),\\ V^{s}_{3,[m]}(z_2) &= V^{+}_{[m]}(z_2) + V^{-}_{[m]}(z_2) - V^{i}_{3,[m]}(z_2),\\ V^{s}_{3,(m)}(z_2) &= V^{+}_{(m)}(z_2) + V^{-}_{(m)}(z_2) - V^{i}_{3,(m)}(z_2).\end{aligned} \tag{34}$$

As to the interpretation of the transformation we note that it is chosen such that $V^{+}_{[m]}$ and $V^{+}_{(m)}$ would represent amplitudes of modes in the reference waveguide travelling in the positive z-direction, while $V^{-}_{[m]}$ and $V^{-}_{(m)}$ would represent amplitudes of modes travelling in the negative z-direction. The resulting differential equations (31) are such that in the reference waveguide the mutual coupling between the modes vanishes and we end up with a system of uncoupled first-order ordinary differential equations.

The fact that the system of differential equations (31), contrary to the system (14), leads to a stable associated initial-value problem, can be explained by studying the value of the elements of the coefficient matrices in these differential equations. It can be shown that the diagonal elements of the matrices $(Z_{(m)(n)})$ and $(Y_{[m][n]})$ are approximately proportional to the square of the cut-off wavenumber of the appertaining mode. This property will cause an appreciable loss of accuracy when the summations in (14) are carried out, expecially for higher-order field components, and as such it is the cause of the instability in the solution of the initial-value problem. As to the elements of the other matrices in (15) and (16) we note that they show no striking dependence on the wavenumber. In (31), the elements of the impedance- and admittance matrices are multiplied by a wave impedance or admittance of a mode in the reference waveguide. Because of this, the diagonal elements of the coefficient matrices in (31) are approximately proportional to the cut-off wavenumber itself of the appertaining modes. Because of this, the summations in (31) do not suffer from an appreciable loss of accuracy and consequently the initial-value problem related to (31) behaves numerically stable. The system of differential equations (31) is referred to as the coupled-mode form [9] of the generalized telegraphist's equations.

5. Discussion of the numerical techniques

In solving the diffraction problem under consideration, numerical difficulties of two different kinds are encountered. The first is posed by the evaluation of the impedances and admittances defined in (15) and (16). The accurate computation of these coefficients is

difficult for those transverse modal functions $T_{[m]}$ and $T_{(m)}$ that oscillate rapidly over the cross-section. For all but the lower-order modes these oscillations are more rapid than the changes in the permittivity and the permeability over the domain occupied by the obstacle. In general, reliable results are achieved in the following way. For a given value of z, the cross-section is divided into subdomains of such size that the medium properties over these subdomains can, with sufficient accuracy, either be assumed to be constant or to vary linearly as a function of the transverse coordinates. The shape of these subdomains is chosen such that, for the transverse modal functions at hand, the double integrations over the former can be carried out analytically. The integral over the cross-section D then follows as the sum of the integrals over the subdomains. In some cases it is possible to write the two-dimensional integral as the product of two one-dimensional integrals. This property simplifies the computations considerably.

The second numerical difficulty lies in the numerical solution of the two-point boundary-value problem defined by the system of differential equations (31), together with the boundary conditions (32) and (33). This two-point boundary-value problem is solved by using the method of invariant imbedding [10]. The exact form of the imbedding that we have employed, it outlined in Appendix A. We have chosen the method of invariant imbedding mainly because of its relative ease to handle general boundary conditions as compared with shooting methods. We have solved the initial-value problems (A.7), (A.8) and (A.9) with the classical fourth-order Runge–Kutta formula [11]. For the integration of (A.12) we have used the Euler–MacLaurin summation formula [12]. All computations have been carried out in single precision arithmetic on the IBM-370/158 computer of the Computing Centre of the Delft University of Technology.

Finally, it follows from (32) and (33) that the square matrices $\boldsymbol{\alpha}$, $\boldsymbol{\beta}$, $\boldsymbol{\gamma}$ and $\boldsymbol{\delta}$ in (A.3) and (A.4) are diagonal ones, which simplifies the solution of (A.15) considerably.

Several checks on the computer program and on the computational results have been carried out in order to eliminate possible inaccuracies and/or errors. We mention some of them.

(1) *Conservation of energy.* In lossless configurations, i.e. when ε and μ are real, the power carried by the incoming field should equal the power carried by the outgoing field. This condition was satisfied to within at least five significant figures.

(2) *Reciprocity.* In reciprocal configurations (to which class our obstacles belong), scattered fields that pertain to two different incident fields should satisfy certain reciprocity relations. These relations were satisfied to within five significant figures.

(3) *Geometrical symmetry.* In many configurations the waveguide and the inhomogeneity present in it show a number of geometrical symmetry properties. Scattered fields associated with suitably chosen incident fields (as far as geometrical symmetry is considered) should reflect the symmetry of the configuration. This condition was satisfied (without having these symmetry properties built in in the numerical procedure, of course).

(4) *Convergence of numerical procedures.* The accuracy of a numerical integration depends on the number of intervals (subdomains) that has actually been chosen. In general, an increase of this number is expected to improve the accuracy of the result and hence to give some insight into the accuracy eventually obtained. Furthermore, we know from numerical analysis the relation between the stepsize and accuracy. The relevant relation proved to be consistent with the one obtained from the actual numerical results.

(5) *Comparison of our results with those that have been obtained by other methods.* Results that are obtained by our method of computation are compared with those that have been reported in papers that deal with other numerical techniques [3, 4, 5, 13, 14], or with experimental results [13, 15]. Our results are found to be in accordance with the computational results from [3], [5] and [14]. Discrepancies have been found between our results and those given in [4] and [13]. More detailed comments on this are given in Section 6.

Finally, we note that the stepsize, the number of subdomains and the number of modes taken into account have been chosen such that our final accuracy proved to be a few percent. For the reference medium we have chosen vacuum i.e. $\varepsilon_0 = 8.8544 * 10^{-12}$, $\mu_0 = 4\pi * 10^{-7}$.

6. Numerical results

In this section numerical results pertaining to three different types of obstacles present in a waveguide of rectangular cross-section are presented. In the waveguide cross-section D we choose a Cartesian coordinate system with its origin at one of the corners. The x- and y-axis are taken in the walls of the waveguide cross-section. Changing to the usual double-subscript notation, the T-functions are [1]

$$\begin{aligned} T_{[m,n]} &= (4\sigma_m\sigma_n/ab)^{\frac{1}{2}}\kappa_{[m,n]}^{-1}\cos(m\pi x/a)\cos(n\pi y/b) \\ &\qquad \text{with } m, n = 0, 1, 2, \ldots, (m, n) \neq (0, 0), \\ T_{(m,n)} &= (4/ab)^{\frac{1}{2}}\kappa_{(m,n)}^{-1}\sin(m\pi x/a)\sin(n\pi y/b) \\ &\qquad \text{with } m, n = 1, 2, 3, \ldots, \end{aligned} \tag{35}$$

where $D = \{x, y | 0 < x < a, 0 < y < b\}$,

$$\kappa_{[m,n]} = \kappa_{(m,n)} = ((m\pi/a)^2 + (n\pi/b)^2)^{\frac{1}{2}} > 0, \tag{36}$$

and

$$\sigma_p = \begin{cases} \frac{1}{2} \text{ when } p = 0, \\ 1 \text{ when } p = 1, 2, \ldots, \end{cases} \tag{37}$$

where a and b denote the sizes of the waveguide in the x- and y-direction, respectively (Fig. 2). Three applications of our method will be given.

(1) *E-plane applicator.* The first configuration we deal with is the so-called E-plane applicator (Fig. 2). An E-plane applicator is a waveguide section of rectangular cross-section, loaded by a dielectric sheet that is parallel to the direction of the electric-field vector. This configuration is applied, amongst others, in drying leather sheets with the aid of microwave power [15]. Neglecting the influence of the slots through which the sheet is transported across the guide, we can consider the leather sheet as a lossy dielectric obstacle that is cylindrical in the y-direction. A longitudinal section of the configuration is shown in Fig. 3. The waveguide used is the WR 284 guide (Table 2). The operating frequency of the incident dominant $TE_{1,0}$-mode, which is travelling in the positive z-direction, is chosen to be 2.45 GHz. The leather sample of thickness c is placed at the centre of the waveguide, hence

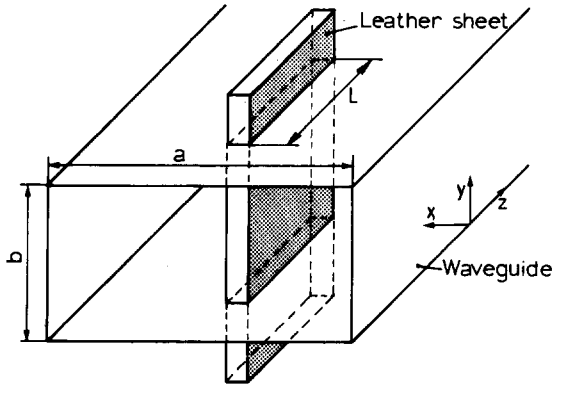

Figure 2. Rectangular waveguide with cylindrical leather sheet [13].

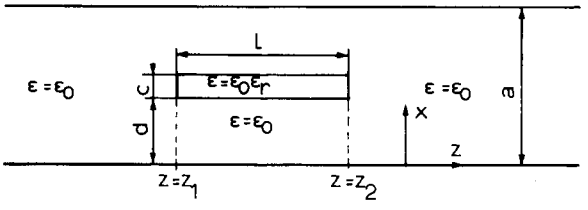

Figure 3. Longitudinal section of *E*-plane applicator [13].

TABLE 2
Dimensions of standard waveguides of rectangular cross-section.

Waveguide designation	Width *a* mm	Height *b* mm
WR 90	22.86	10.16
WR 284	72.14	34.04

TABLE 3
Results for wet leather samples of thickness 2.5 mm in a WR 284 waveguide at 2.45 GHz.

Moisture percentage on wet basis	Length mm	$\varepsilon = \varepsilon' - j\varepsilon''$		Reflection factor, dB			Transmission factor, dB		
		ε'	ε''	Bhartia measured	Bhartia computed	Our results	Hamid measured	Bhartia computed	Our results
0.0	90.2	2.01	0.118	9.2	8.88	27.3	0.29	0.273	0.291
7.8	94.0	2.23	0.182	9.6	9.39	30.7	0.46	0.485	0.455
18.8	96.5	3.58	0.783	12.3	12.64	23.4	1.9	1.975	1.92
38.8	99.3	10.68	3.361	6.42	6.42	8.51	7.3	7.27	7.48
57.3	99.6	29.46	8.888	4.6	4.68	5.10	19.4	19.13	20.5

$d = (a - c)/2$ (see Fig. 3). Since the configuration is cylindrical in the y-direction and the incident field is independent of y, only $TE_{m,0}$-fields, $m = 1, 2, \ldots$, will be excited. In Table 3 our results are compared with the experimental results of Hamid et al. [15] and with the experimental and computational results of Bhartia [13]. The results for the transmission factors agree favourably. For the reflection factors however our results differ considerably from those of Bhartia. For those of his leather samples that have a moisture content of 0% and 7.8% it can be shown that the total power carried by the reflected and the transmitted field (as obtained from Bhartia's results) exceeds the incident power and this violates the law of conservation of energy. Therefore, the reflection factors presented in [13] are expected to be in error.

In our computations the number of modes that has been taken into account runs from five to eleven; the higher the permittivity of the leather sample, the larger the number of modes that is needed in the computation. The relevant computation time amounts from about ten seconds for five modes to eighty seconds for eleven modes.

(2) *Cylindrical plasma column of variable electron density.* The second configuration to be considered is shown in Fig. 4. A circularly cylindrical plasma column of radius ρ is placed parallel to the narrow side (y-direction) of a rectangular waveguide. The axis of the plasma column is located at $x = a/2$, $z = 0$. The plasma column is assumed to have a radially varying electron density distribution of the form

$$n(r) = n_0(1 - \alpha r^2/\rho^2), \tag{38}$$

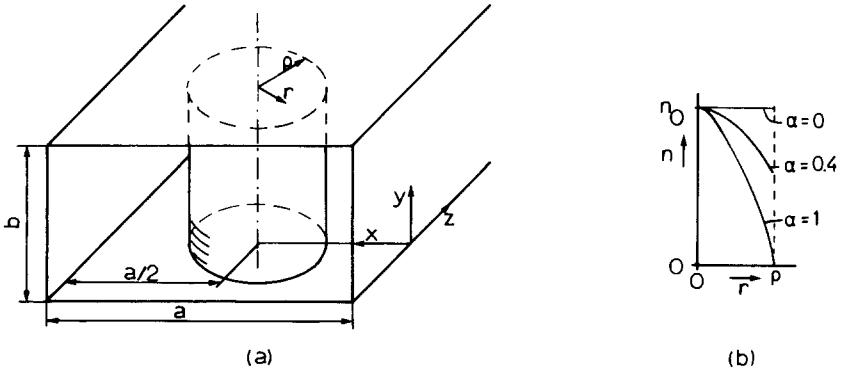

Figure 4. Cylindrical plasma column in a rectangular waveguide (a) and electron density profile (b) [14].

TABLE 4
The values of $\omega_{p,0}$, α *and* ν *taken from* [14].

α	$\omega_{p,0}$ (rad/s)	ν (Hz)
1	$67.5 * 10^9$	$3.5 * 10^9$
0.4	$50.5 * 10^9$	$1.6 * 10^9$
0	$45.0 * 10^9$	$1.0 * 10^9$

where n_0 denotes the electron density on the axis of the column, r denotes the radial distance from a point in the column to its axis and α is a parameter ($0 \leq \alpha \leq 1$) whose value determines the electron density profile. The relative permittivity ε_r of such a plasma column can be written [16] as

$$\varepsilon_r = 1 - \omega_{p,0}^2(1 - \alpha r^2/\rho^2)/(\omega(\omega - j\nu)), \tag{39}$$

where $\omega_{p,0}$ denotes the plasma frequency corresponding to an electron density n_0, and ν denotes the collision frequency. The waveguide used is the WR 90 guide (Table 2). For the incident field we take the dominant $TE_{1,0}$-mode travelling in the positive z-direction. A configuration of this kind is used for microwave plasma diagnostics [14]. Since the configuration is cylindrical in the y-direction and the incident field is independent of y, only $TE_{m,0}$-fields, $m = 1, 2, \ldots$, are excited. In Fig. 5, the modulus $|R|$ of the reflection factor R of the dominant mode and the value of $\arg(R)/\pi$ are plotted as a function of the frequency f for a plasma column with $\rho = 10$ mm, and for several values of α. The values of $\omega_{p,0}$ and ν that have been chosen are listed in Table 4, and have been taken from [14]. A good agreement between our results and those of Cupini et al. [14] is observed and consequently an efficient curve fitting method for the plasma diagnostic purposes can easily be realized by using our computer program. The computations have been performed by taking into account only three modes. The computation time amounts to about five seconds for a single problem.

Next, we replace the plasma column by a column the axis of which is parallel to the broad side (x-direction) of the waveguide and located at $y = b/2$, $z = 0$. For the incident field we again take the dominant $TE_{1,0}$-mode travelling in the positive z-direction. Since the

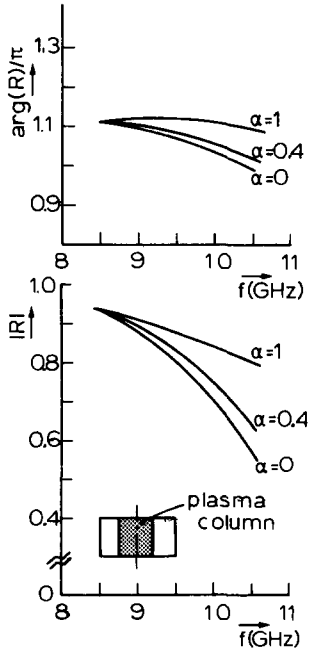

Figure 5. Values of $|R|$ and $\arg(R)/\pi$ as a function of the frequency f and the parameter α (axis of the plasma column in the y-direction), $\rho = 10$ mm.

configuration is cylindrical in the x-direction, the fields in the waveguide will show the same x-dependence as the incident field. Therefore only $TE_{1,m}$-fields $m = 0, 1, 2, \ldots$, and $TM_{1,m}$-fields, $m = 1, 2, \ldots$, will be excited. In Fig. 6 the modulus $|R|$ of the reflection factor of the dominant mode and the value of $\arg(R)/\pi$ are plotted as a function of the frequency f for several values of the radius ρ and for $\alpha = 0.4$. The values of $\omega_{p,0}$ and ν are taken from Table 4. The computations have been performed taking into account five TE-modes and four TM-modes. As an example we mention that the computation time for $\rho = 5$ mm is about fifty seconds for a single problem.

(3) *Pyramidal waveguide termination.* The third configuration to be considered is the leaning pyramidal waveguide termination in a WR 90 guide. The configuration to be investigated is depicted in Fig. 7. A configuration of this kind is used to simulate a reflectionless waveguide termination. The square base of the pyramid is cemented to a perfectly conducting shorting plug at the plane $z = 0$. The side length of the base of the pyramid is $d = b = 10.16$ mm. One side of the pyramid, which has a length L, is cemented to the broad side of the waveguide wall for maximum mechanical strength and maximum heat dissipating capability. The inhomogeneous region, in which the field is described with the aid of the "Generalized Telegraphist's Equations", is taken to be the region $(z_1, z_2) = (-L, 0)$. As a consequence of the shorting plane at $z = 0$, the boundary condition (33) at $z = z_2$ should be replaced by

$$\begin{aligned} V^+_{[m]}(z_2) + V^-_{[m]}(z_2) &= 0, \\ V^+_{(m)}(z_2) + V^-_{(m)}(z_2) &= 0. \end{aligned} \tag{40}$$

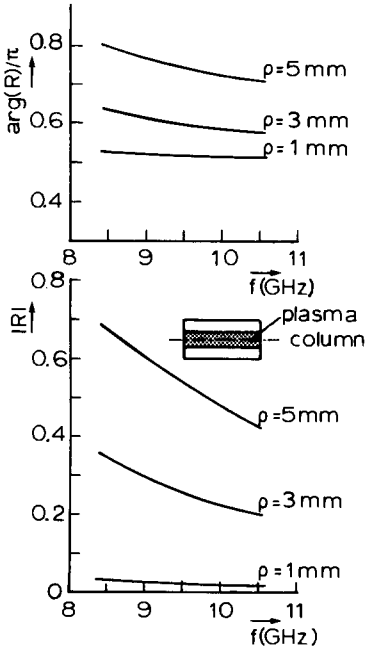

Figure 6. Values of $|R|$ and $\arg(R)/\pi$ as a function of the frequency and the radius ρ, (axis of the plasma column in the x-direction), $\alpha = 0.4$.

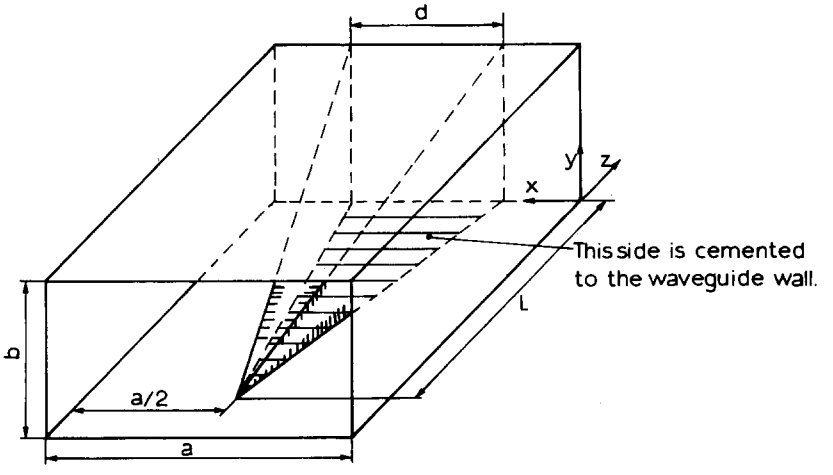

Figure 7. Pyramidal waveguide termination cemented to the waveguide wall.

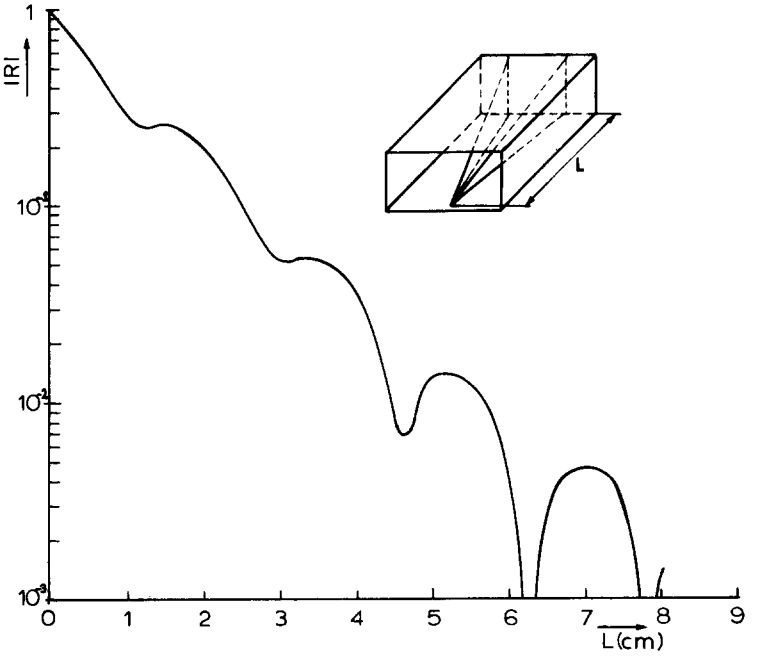

Figure 8. Modulus of the reflection factor as a function of the length of a pyramidal waveguide termination, $\varepsilon_r = 2.2$, $\mu_r = 1 - 1.25j$, $f = 9.84$ GHz.

The pyramidal waveguide termination is made of lossy material with real relative permittivity $\varepsilon_r = 2.2$ and complex relative permeability $\mu_r = 1 - 1.25j$ which properties are approximately those of ECCOSORB MF-117 as provided by the manufacturer. The operating frequency of the incident dominant $TE_{1,0}$-mode, which is travelling in the positive z-direction, is taken to be 9.84 GHz. In Fig. 8 the modulus $|R|$ of the reflection factor R is plotted as a function of the length L. In our calculations we have taken into account seven

TE-modes, viz. $TE_{i,j}$, $i = 0, 1, 2, 3$, $j = 0, 1$, $(i,j) \neq (0,0)$ and three *TM*-modes viz. $TM_{i,1}$, $i = 1, 2, 3$. The computation time for $L = 45$ mm is 150 seconds.

7. Conclusion

In this paper an exact method is described for computing numerically the scattering properties of an inhomogeneity present in a cylindrical waveguide. Scattering configurations of various degrees of complexity are investigated, using a computer program that is based on this method. As compared with other methods, the present method requires, in general, a relatively small amount of computation time and storage capacity. Another advantage of the method is its flexibility. For a specific problem only a subroutine for the computation of the coupling integrals in (15) and (16) needs to be written, the remaining part of the program being unchanged. For obstacles that show strong local variations in their permittivity and/or permeability, a large number of modes has to be taken into account in order to arrive at the desired accuracy and this, even with our method, leads to considerable computation times and storage requirements. But then, no alternative is available either. Another limitation seems to be that the method cannot be generalized to problems involving perfectly conducting obstacles. For the latter type of obstacles, the integral-equation method still seems to be the only method of a general kind.

Acknowledgement

The author wishes to thank Professor A. T. de Hoop for his suggestions and stimulating discussions concerning the research presented in this paper.

Appendix A. The method of invariant imbedding

For the theory of the method of invariant imbedding to solve systems of ordinary differential equations numerically, we refer to Scott [10]. In this appendix we shall present the set of invariant-imbedding equations pertinent to the solution of the system of differential equations (31), together with the boundary conditions (32) and (33). Let us consider the system of differential equations

$$\partial_z \boldsymbol{u}(z) = \boldsymbol{A}(z)\boldsymbol{u}(z) + \boldsymbol{B}(z)\boldsymbol{v}(z), \qquad z_1 < z < z_2, \tag{A.1}$$

$$-\partial_z \boldsymbol{v}(z) = \boldsymbol{C}(z)\boldsymbol{u}(z) + \boldsymbol{D}(z)\boldsymbol{v}(z), \qquad z_1 < z < z_2. \tag{A.2}$$

In (A.1) and (A.2), $\boldsymbol{u}(z)$ and $\boldsymbol{v}(z)$ denote unknown z-dependent n-vectors, $\boldsymbol{A}(z)$, $\boldsymbol{B}(z)$, $\boldsymbol{C}(z)$ and $\boldsymbol{D}(z)$ denote known z-dependent $n \times n$ matrix functions. The system of differential equations is subject to the boundary conditions

$$\boldsymbol{\alpha u}(z_1) + \boldsymbol{\beta v}(z_1) = \boldsymbol{\varepsilon}_1, \tag{A.3}$$

$$\boldsymbol{\gamma u}(z_2) + \boldsymbol{\delta v}(z_2) = \boldsymbol{\varepsilon}_2. \tag{A.4}$$

In (A.3) and (A.4), $\boldsymbol{\alpha}$, $\boldsymbol{\beta}$, $\boldsymbol{\gamma}$ and $\boldsymbol{\delta}$ are known $n \times n$ matrices and $\boldsymbol{\varepsilon}_1$ and $\boldsymbol{\varepsilon}_2$ are known n-vectors.

The functions and constants introduced above, are in general complex-valued. We shall assume that the system of differential equations (A.1), (A.2), together with the boundary conditions (A.3), (A.4), has a unique solution. We now introduce the Ricatti and recovery transformations through the relations

$$\boldsymbol{u}(z) = \boldsymbol{R}_1(z)\boldsymbol{v}(z) + \boldsymbol{R}_2(z)\boldsymbol{u}(z_1), \tag{A.5}$$

$$\boldsymbol{v}(z_1) = \boldsymbol{Q}_1(z)\boldsymbol{v}(z) + \boldsymbol{Q}_2(z)\boldsymbol{u}(z_1). \tag{A.6}$$

In (A.5) and (A.6), $\boldsymbol{R}_1(z)$, $\boldsymbol{R}_2(z)$, $\boldsymbol{Q}_1(z)$ and $\boldsymbol{Q}_2(z)$ are complex-valued, z-dependent $n \times n$ matrix functions that are defined through the differential equations

$$\partial_z \boldsymbol{R}_1(z) = \boldsymbol{B}(z) + \boldsymbol{A}(z)\boldsymbol{R}_1(z) + \boldsymbol{R}_1(z)(\boldsymbol{D}(z) + \boldsymbol{C}(z)\boldsymbol{R}_1(z)), \tag{A.7}$$

$$\partial_z \boldsymbol{R}_2(z) = (\boldsymbol{A}(z) + \boldsymbol{R}_1(z)\boldsymbol{C}(z))\boldsymbol{R}_2(z), \tag{A.8}$$

$$\partial_z \boldsymbol{Q}_1(z) = \boldsymbol{Q}_1(z)(\boldsymbol{C}(z)\boldsymbol{R}_1(z) + \boldsymbol{D}(z)), \tag{A.9}$$

$$\partial_z \boldsymbol{Q}_2(z) = \boldsymbol{Q}_1(z)\boldsymbol{C}(z)\boldsymbol{R}_2(z), \tag{A.10}$$

together with the initial conditions

$$\boldsymbol{R}_1(z_1) = \boldsymbol{0},\ \boldsymbol{R}_2(z_1) = \boldsymbol{1},\ \boldsymbol{Q}_1(z_1) = \boldsymbol{1},\ \boldsymbol{Q}_2(z_1) = \boldsymbol{0}, \tag{A.11}$$

that are in accordance with (A.5) and (A.6) at $z = z_1$.

Now, the initial-value problem defined by (A.7)–(A.11) can be solved in a straightforward manner, for instance by using a Runge–Kutta method. We note that (A.10) can be solved by first rewriting it as

$$\boldsymbol{Q}_2(z) = \int_{\zeta=z_1}^{z} \boldsymbol{Q}_1(\zeta)\boldsymbol{C}(\zeta)\boldsymbol{R}_2(\zeta)\mathrm{d}\zeta, \tag{A.12}$$

where we have used (A.11). The integration in (A.12) can be carried out easily. Having solved the initial-value problem, $\boldsymbol{R}_1(z_2)$, $\boldsymbol{R}_2(z_2)$, $\boldsymbol{Q}_1(z_2)$ and $\boldsymbol{Q}_2(z_2)$ are known and we arrive at expressions containing the still unknown quantities $\boldsymbol{u}(z_1)$, $\boldsymbol{v}(z_1)$, $\boldsymbol{u}(z_2)$ and $\boldsymbol{v}(z_2)$ by using (A.5) and (A.6) at $z = z_2$. We obtain

$$\boldsymbol{u}(z_2) = \boldsymbol{R}_1(z_2)\boldsymbol{v}(z_2) + \boldsymbol{R}_2(z_2)\boldsymbol{u}(z_1), \tag{A.13}$$

$$\boldsymbol{v}(z_1) = \boldsymbol{Q}_1(z_2)\boldsymbol{v}(z_2) + \boldsymbol{Q}_2(z_2)\boldsymbol{u}(z_1). \tag{A.14}$$

Now, (A.3), (A.4), (A.13) and (A.14) constitute a system of four equations from which the unknown vectors $\boldsymbol{u}(z_1)$, $\boldsymbol{v}(z_1)$, $\boldsymbol{u}(z_2)$ and $\boldsymbol{v}(z_2)$ can be solved. Upon elimination of $\boldsymbol{u}(z_1)$ and $\boldsymbol{v}(z_2)$ we obtain a result that can be written as

$$\begin{pmatrix} \mathbf{1} + \boldsymbol{R}_1(z_2)\boldsymbol{\delta}^{-1}\boldsymbol{\gamma} & \boldsymbol{R}_2(z_2)\boldsymbol{\alpha}^{-1}\boldsymbol{\beta} \\ \boldsymbol{Q}_1(z_2)\boldsymbol{\delta}^{-1}\boldsymbol{\gamma} & \mathbf{1} + \boldsymbol{Q}_2(z_2)\boldsymbol{\alpha}^{-1}\boldsymbol{\beta} \end{pmatrix} \begin{pmatrix} \boldsymbol{u}(z_2) \\ \boldsymbol{v}(z_1) \end{pmatrix} =$$

$$= \begin{pmatrix} \boldsymbol{R}_2(z_2)\boldsymbol{\alpha}^{-1} & \boldsymbol{R}_1(z_2)\boldsymbol{\delta}^{-1} \\ \boldsymbol{Q}_2(z_2)\boldsymbol{\alpha}^{-1} & \boldsymbol{Q}_1(z_2)\boldsymbol{\delta}^{-1} \end{pmatrix} \begin{pmatrix} \boldsymbol{\varepsilon}_1 \\ \boldsymbol{\varepsilon}_2 \end{pmatrix}. \tag{A.15}$$

From (A.15), $\boldsymbol{u}(z_2)$ and $\boldsymbol{v}(z_1)$ can be solved and finally $\boldsymbol{u}(z_1)$ and $\boldsymbol{v}(z_2)$ can be obtained using (A.3) and (A.4), respectively.

REFERENCES

[1] S. A. Schelkunoff, Generalized Telegraphist's equations for waveguides, *Bell Syst. Techn. J.*, vol. 31 (1952) 784–801.

[2] N. Marcuvitz, *Waveguide Handbook*, New York, McGraw-Hill, 1951, pp. 266.

[3] G. de Jong and W. Offringa, Reflection and transmission by a slant interface between two media in a rectangular waveguide, *Int. J. Electronics* 34 (1973) 453–463.

[4] Y. L. Chow and S.-C. Wu, A moment method with mixed basis functions for scattering by waveguide junctions, *IEEE Trans. on MTT*, vol. MTT-21 (1973) 333–340.

[5] S. Caorsi, G. Cicconi and C. Rosatelli, Calcolo di alcune discontinuita in guida d'onda mediante funzioni di Green, *Alta frequenza*, Vol. XLV (1976) 64–71.

[6] G. Mur, D. Quak and G. J. van Dijk, Computational aspects of the scattering of electromagnetic waves by a dielectric obstacle in a waveguide of rectangular cross-section, *Conference paper, International Conference on Numerical Methods in Electrical and Magnetic Field Problems*, S. Margherita Ligure (Italy), June 1–4, 1976.

[7] S. M. Roberts and J. S. Shipman, *Two-point boundary value problems: Shooting Methods*, New York, American Elsevier, 1972, pp. 6, Chapter 2.

[8] H. B. Keller, *Numerical methods for two-point boundary-value problems*, Waltham, Blaisdell Publishing Company, 1968, pp. 39, Chapter 2.

[9] W. H. Louisell, *Coupled mode and parametric electronics*, New York, John Wiley & Sons, 1960, pp. 21.

[10] M. R. Scott, *Invariant imbedding and its applications to ordinary differential equations*, Reading, Massachusetts, Addison–Wesley Publishing Company, 1973, pp. 174.

[11] M. R. Scott, *Invariant imbedding and its applications to ordinary differential equations*, Reading, Massachusetts, Addison–Wesley Publishing Company, 1973, pp. 31.

[12] E. Isaacson and H. B. Keller, *Analysis of numerical methods*, New York, John Wiley & Sons, 1966, pp. 287.

[13] P. Bhartia, Evaluation of parameters for the *E*-plane applicators, *Proc. IEE* 122 (1975) 267–269.

[14] E. Cupini, V. G. Molinari and P. Poli, Reflection coefficient of an electromagnetic wave by a plasma column of variable electron density in a waveguide, *Alta Frequenza*, Vol. XLII, P. 62–2E, 1973.

[15] M. A. K. Hamid, S. S. Stuchly, P. Bhartia and N. Mostowy, Microwave drying of leather, *J. Microwave Power*, 7 (1972) 43–49.

[16] V. H. Weston, Kinetic theory of scattering by a plasma cylinder, *Journ. Math. Phys.*, 13 (1972) 1443–1450.